Settling Behaviors of Iron Oxide Suspensions

G. G. Glasrud, R. C. Navarrete, L. E. Scriven, and C. W. Macosko
Center for Interfacial Engineering and Dept. of Chemical Engineering and Materials Science, University of Minnesota, Minneapolis, MN 55455

This article shows the settling behaviors of flocculated, magnetic and nonmagnetic iron oxide suspensions. It is unique, since in the literature on settling of model submicron flocculated particulate suspensions there is no direct visualization of the structures and how they change during settling. Channeling, cracking, and a novel collapse phenomenon were detected during settling. Causes were investigated using lapse videorecording for side and top views. The effect of air bubbles was shown to contribute to the accelerated settling of the suspension by creating channels that conduct oil to the settling front. Settling heights were recorded for long periods of time (up to a year) for iron oxide suspensions of different concentrations. Decreasing tube diameters delayed settling, and magnetic interparticle forces produced smaller final settling heights. The effect of magnetic forces was interpreted in terms of a floc model. The model finds magnetic flocs 1.3 to 1.4 times denser than their nonmagnetic analogs. Finally, a mechanism is put forth to interpret the settling behavior observed.

Introduction

The main purpose of documenting the settling behavior of the iron oxide suspensions is to marshall the information that such behavior provides about the *structures* formed by the particles in suspension.

By structure we mean a semipermanent association of particles, particle aggregates, particle flocs, or in general, structural units that have some capacity to develop resisting force in response to their deformation.

The documentation here is unique, for in the literature on settling of model submicron flocculated particulate suspensions there is no direct visualization of the structures and how they change during settling. Prior work was based on indirect visualization techniques such as X-ray probing (Gaudin et al., 1959; Somasundaran et al., 1987), light attenuation (Allen, 1987), and ultrasound (Wedlock et al., 1990; Howe and Robins, 1990), together with simple theories—free falling sphere in Stokes flow at the dilute limit and flow through a packed bed at the concentrated limit—and intuition (Davies and Kaye, 1971; Ayoub et al., 1983; Hietala and Smith, 1989, to mention some). These techniques did not reveal clearly the mechanisms that underlie settling of the type of suspensions of interest here.

Settling of flocculated suspensions is not well understood, given that flocculated suspensions do not fit the definition of dilute suspensions, where particles behave as independent flow units, and concentrated suspensions, where the translational and rotational degrees of freedom of the particles are severely restricted. Michaels and Bolger (1962), Buscall (1982), Tiller and Khatib (1984), and Buscall and White (1987) have proposed macroscopic theories for these systems that do not take into account the mechanisms that occur at the particle level during settling, but are vital to understand the macroscopic settling behavior of flocculated suspensions, as is demonstrated here. On the other hand, simulations resembling molecular dynamics have been widely used to elucidate the particle-particle mechanisms underlying settling of concentrated suspensions, but they have been either focused on the effect of Brownian forces (Dickinson and Parker, 1984; Ansell and Dickinson, 1987; Huang and Somasundaran, 1988; Dickinson, 1989) or on hydrodynamic interactions (Shih et al., 1987; Phillips et al., 1988; Brady et al., 1988; Koch and Shaqfeh, 1989); no emphasis has been put on interparticle interactions.

More complete reviews of past theoretical and experimental works on sedimentation of flocculated suspensions have been published by Somasundaran (1981), Dickinson (1989), and Buscall (1990). The work that pertains most to the observations reported in this article is that of Somasundaran and co-workers (Somasundaran et al., 1975; Harris et al., 1975; Nagaraj et

Correspondence concerning this article should be addressed to C. W. Macosko.
Present address of G. G. Glasrud: Mandan Refinery, P.O. Box 5000, Mandan, ND 58554.
Present address of R. C. Navarrete: Dowell Schlumberger Inc., P.O. Box 2710, Tulsa, OK 74101.

al., 1977; Somasundaran, 1981). They measured settling of phosphate slimes, which are water based suspensions of submicron particles generated as a byproduct in the production of fertilizer. Among the components present in the slimes are phosphate minerals, quartz, clay, attapulgite and wavellite. The slimes are stored in tanks and accumulate with time. The settling rates are so small that it can take decades before any appreciable separation is achieved. Somasundaran and coworkers studied methods to accelerate the settling of these systems by means of additives, air bubbles and coarse particles (32 μm to 990 μm). In the process they found that the effect of air bubbles and coarse particles is to produce channels from which the water rises to the top. They also observed the formation of water cavities in the bulk structure of the slime and microvolcanos at the surface of the settling front. They did not indicate the dimensions of the channels and the cavities. Based on these observations they proposed a phenomenological interpretation of the settling height vs. time curves—that showed a S-shape—in which the tendency of the particles to form a network was taken into account. No visual documentation of these phenomena was presented. To our knowledge there are no other works in the literature that described similar phenomena.

There are few works that report nonhomogeneous sedimentation. Allen and Uhlherr (1989) reported nonhomogeneous sedimentation of suspensions of glass spheres of average sizes of 0.51 mm and 1.0 mm in a polymer solution, that is, moderately shear thinning (power law index of between 0.6–0.8) viscoelastic suspending media. Typical particle volume fractions were around 40%. This system has a small density difference and low Reynolds numbers. Allen and Uhlherr reported striking patterns of rising liquid pockets, which resemble bubbling fluidization within a progressively compacting bed. Inhomogeneities in particle concentration became increasingly apparent with rising shear-thinning. No inhomogeneities were detected on a similar system suspended in a Newtonian fluid. Allen and Uhlherr's visual observations were reported by means of hand tracing of photographs, that is, original photographs are transformed into dotted patterns, where contrast is represented by different concentrations of dots. This work attributes the nature of the nonhomogeneous behavior purely to the rheological nature of the suspending media.

Our study emphasizes both visualization of the particle structure during settling and measurement of the settling heights for long periods of time (up to a year) in iron oxide suspensions of different concentrations. Channeling, cracking and a novel collapse phenomenon were detected during settling. Causes were investigated using a lapse videotape recording for side and top views. The effect of air bubbles was documented and the effect of the tube diameter and the magnetic forces was demonstrated. Final settling properties were used to obtain floc particle densities.

A mechanism is put forth to interpret the settling behaviors observed.

Experimental

The experimental suspension system consisted of needle-like particles of iron oxide suspended in mineral oil. The particle density was 4.5 g/cm^3. The average length of the particles was about 0.5 μm and the average length to diameter ratio was 5; transmission electron micrographs of similar particles were published by Yang et al. (1986). The liquid medium was heavy mineral oil from Sergent-Welch Co., with viscosity of about 135 cp (25°C) and density of 0.863 g/cm^3. The iron oxide particles were treated with an alkoxysilane surfactant, which reacted with the hydroxyl sites on the surface of the particles to prevent particle aggregation by chemical bonding (Utsugi et al., 1985). In order to study the effect of magnetic interactions, two crystalline forms of this system were used, that is, γ-Fe_2O_3 which is ferromagnetic and is usually used as a recording medium in audiotapes and videotapes, and α-Fe_2O_3, the nonmagnetic analog version of the iron oxide particles. The demagnetized analog, α-Fe_2O_3, was prepared by heat treatment of the magnetic form above the Curie temperature, typically 600°C for 1 h. Therefore, the nonmagnetic powder should have the same size and shape distributions.

A ball mill was employed for the preparation of the suspensions. Mill vessels were plastic bottles 6 cm in diameter, and milling media were 9.5 mm steel balls. Powder was mixed with the mineral oil in a 40 weight % (11.3% by volume) concentration and then milled for 24 h. This suspension was then diluted to several concentrations.

The settling experiments were carried out in flat-bottom round glass test tubes at 20–27°C. Test tube inside diameters were 20 mm (10 mm in some cases), and their length was 100 mm.

The general procedure was to videotape the settling of the suspension in a test tube, then to play back the videotape and measure the height of the interface between the oil-rich region and the particle-rich region as a function of time. Height is defined as the distance between the bottom inside face of the test tube and the interface between the oil-rich region and the particle-rich region.

The experimental procedure consisted of:

- A well-stirred suspension of known concentration was poured into a flat bottom test tube to a height of approximately 80 mm and a diameter of 20 mm.
- The visualization equipment consisted of a Panasonic WV-1350A TV videocamera attached to a Panasonic AG-6050 time lapse videorecorder and monitor (Panasonic Inc., 425 Algonquin Rd., Arlington Heights, IL 60005). Lenses were used with the video camera, which allowed the image to be magnified from 6× to 60×. The image was recorded sideways in order to measure the oil-rich/particle-rich region interface with a videomicrometer upon playback. The image was magnified and focused such that the total height of the suspension appeared as large and clear as possible on the monitor. Fiber optics and a photographer's lamp were also used to enhance the image. After the image was focused properly, a ruler of fine divisions was placed just to the side of the test tube for a few minutes during the beginning of recording; this served as the means for calibrating the videomicrometer.
- The suspension's settling was recorded for about 48 h. After videotaping, the test tube was placed in an immobile test tube rack; the height of the oil-rich/particle-rich region interface was measured with a ruler once a day for the remaining first 100 h of settling, once a week for the next several months, and once a month until the suspension ceased settling.
- The videotape was played back and the height of the oil rich phase-particle-rich region interface was measured with a System VMS videomicrometer from Technical Instrument Company.

Results

The raw data are presented in terms of a compressive strain, defined by:

$$\epsilon_c \equiv \text{Settling Front Height/Total Initial Height} \qquad (1)$$

vs. time; these data are referred to as the settling curve.

Figure 1 presents the settling curves of magnetic suspensions of volume fraction 0.2–9.4% and nonmagnetic suspensions of volume fraction 1.0–6.0%. The general trend in both magnetic and nonmagnetic suspensions indicates a slow settling rate (slope magnitude of the settling curve) during an initial period of time that depends on concentration, followed by a rise in settling rate, which is larger the lower the concentration. The settling rate then falls and approaches zero, that is, the suspension ceases to settle under gravity. The lower the concentration, the smaller the compressive strain when settling ceases.

Magnetic suspensions

The 9.4% volume fraction magnetic suspension settled very little over the first 2,000 h; however, its settling rate appeared to begin rising slightly at about 200 h. This settling curve is incomplete, yet shows the early signs of following the general trend. The 6.0%, 3.3%, 2.3%, and 1.9% volume fraction magnetic suspensions also followed the same general trend and tend towards a final settled state. The 0.2% and 1.0% volume fraction magnetic suspensions followed the general trend and reached a state in which no further settling occurred. The 0.2% and 1.0% curves are significant in that they both show a sudden and dramatic drop in the particle-rich region height; this sharp increase in settling rate is much greater than seen in any other higher concentration.

The videotape recording of the 1.0% volume fraction magnetic suspension revealed the following settling behavior:

(1) The suspension appears homogeneous immediately after loading into the test tube. Figure 2 presents time-lapse photographs of the settling process.

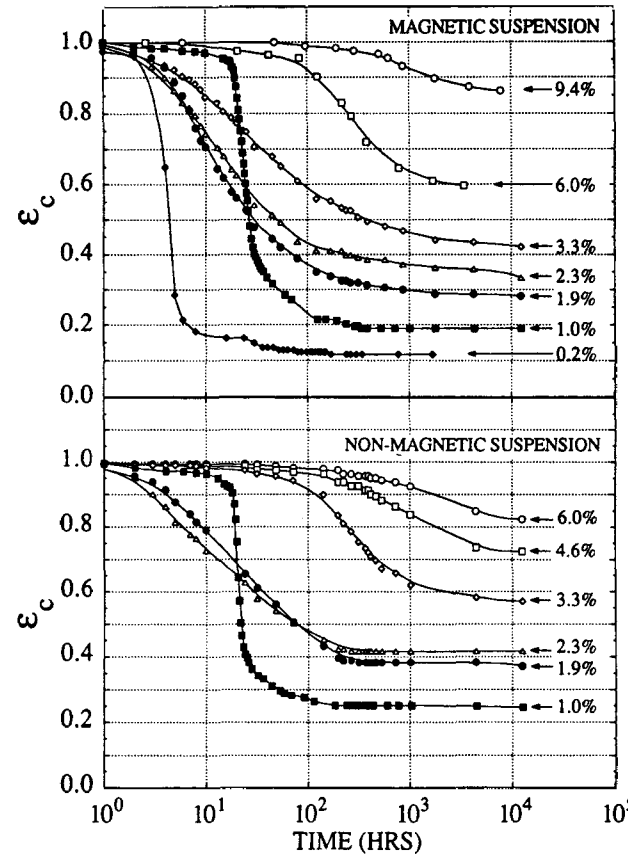

Figure 1. Settling curves of Fe_2O_3 suspensions of indicated concentrations.

(2) After 2 h and 48 min a distinct interface between an oil-rich/particle-rich region develops; the particle-rich region still appears homogeneous at this time.

(3) Cracks of macroscopic dimensions—500 μm–1,000 μm—appear 5–7 h after loading; the cracks are first observed in the upper half of the particle-rich region, and the majority are

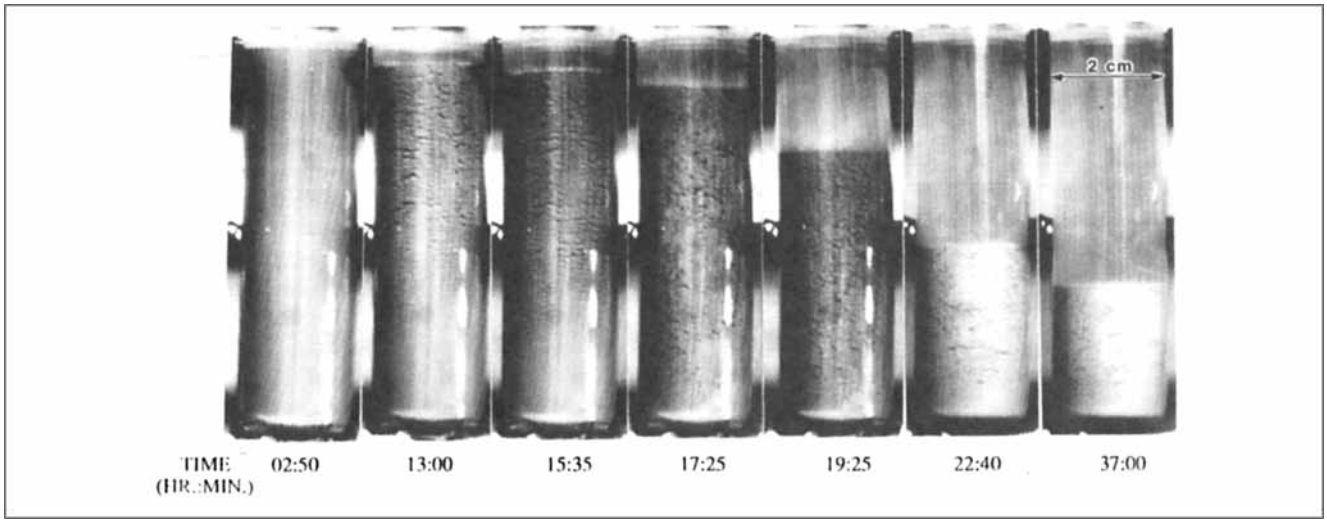

Figure 2. Side-by-side time-lapse photographs of the settling of a 1.0% by volume magnetic iron oxide suspension.

oriented horizontally. Figure 2 shows the suspension after cracks formed at 13 h of settling.

(4) As time increases more cracks appear in the lower half of the particle-rich region, as shown in Figure 2 at 17 h, 25 min of settling. The settling up to this time has proceeded such that the height of the interface between the oil-rich region and the particle-rich region uniformly decreased, no local movement within the particle-rich region was observed; by local movement is meant visible deviations in settling or settling rate among adjacent parts of the suspension.

(5) Local movement is observed in the particle-rich region between 10 and 20 h (~18 h in the footage presented); this local disturbance triggers global rearrangement and collapse of the particle-rich region. Significant macroscopic recirculation and backflow are observed in the particle-rich region during the collapse, as sketched in Figure 3; Figure 2 depicts the beginning of collapse between 17 h, 25 min and 19 h, 25 min.

(6) As the collapse propagates, particles amass at the bottom of the test tube in a reordered structure; this structure is much more compact than the particle-rich region previous to collapse, yet it contains crack-like structures which may be a result of inefficient packing upon collapse. Figure 2 depicts the suspension 22 h and 40 min after loading; at this time the collapse is near an end.

(7) As visible movement within the particle-rich region slows and halts, settling continues in the same manner as it did before collapse occurred. During the next 80 h the cracks compact and disappear; the particle-rich region approaches a final height such that no further settling is observed under gravity.

Similar results were observed in the 0.2% by volume magnetic suspension, the only differences being that this sample collapsed in a shorter time of collapse and to a smaller final settled height.

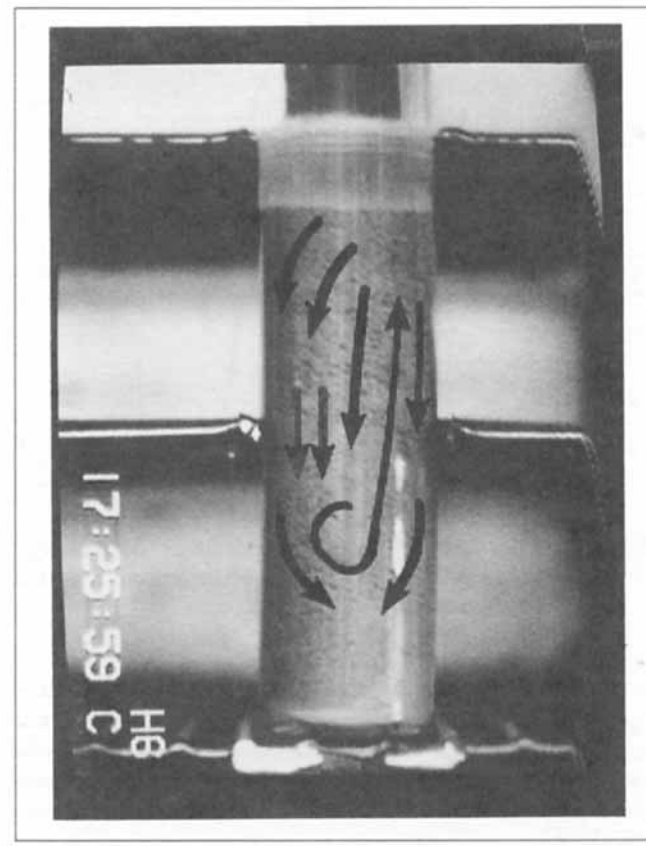

Figure 3. Recirculation and backflows observed during the collapse of a 1.0% by volume γ-Fe_2O_3 suspension.

Nonmagnetic suspension

The shapes of the settling curves of nonmagnetic suspensions are similar to those of their magnetic counterparts. However, there are some differences.

Figure 4 compares magnetic and nonmagnetic settling data for volume fractions of 6.0%, 3.3%, 2.3% and 1.0%, respectively. The general settling behaviors of low concentration nonmagnetic suspensions (1.0% and 2.3% volume fraction) are very similar to that of the respective magnetic suspensions; in fact the 1.0% volume fraction nonmagnetic suspension settles in the same manner as described for the 1.0% magnetic suspension. The higher concentrations (3.3% and 6.0% volume fraction) differ significantly; magnetic suspensions settle faster than their nonmagnetic counterparts. One generalization evident for all initial concentrations greater than 1.0% by volume is that the ratio of final settled height to total initial height is greater for nonmagnetic suspensions.

Effect of tube diameter

Figures 5 show the settling curves for 6.0%, 2.3%, 1.9% and 1.0% volume fraction magnetic suspensions respectively in tubes of two different diameters: 10 mm and 20 mm. These results indicate that a smaller diameter delays the settling curves, that is, it shifts the curves to the right. The effect is significant at high particle concentrations (6%), and it is negligible at low particle concentrations (1.0%). The effect of the wall is to produce shear deformation on the suspension in the vicinity of the wall; thus smaller diameters increase the ratio of sheared suspension to nonsheared suspension. These results are consistent with the systems' rheological behavior. A drastic fall

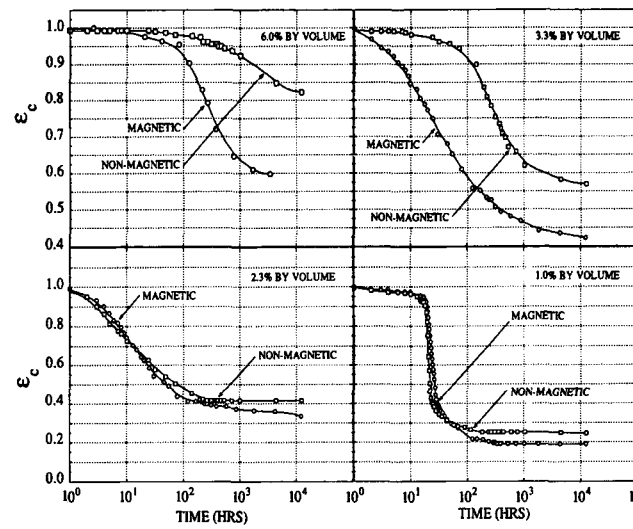

Figure 4. Comparison between magnetic and nonmagnetic Fe_2O_3 settling curves.

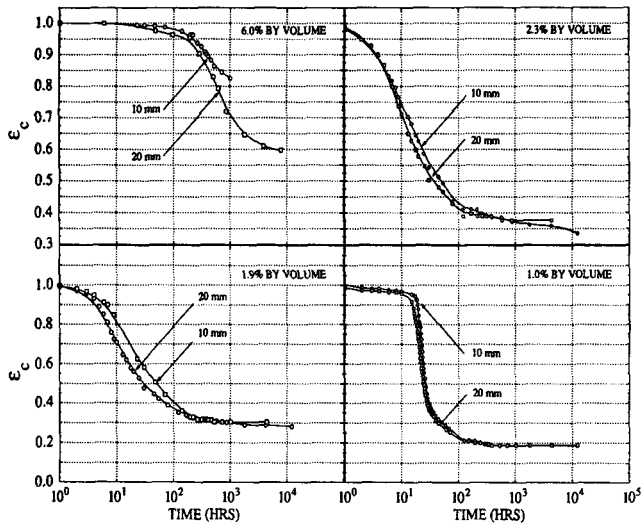

Figure 5. Effect of test tube diameter on settling curves of γ-Fe_2O_3 suspensions of indicated particle volume fractions.

in shear viscosity with increasing shear stress is observed in high concentration magnetic iron oxide suspensions (9.4% and 6.0%) compared to a much milder fall in shear viscosity with increasing shear stress observed in low concentration magnetic iron oxide suspensions (1.9% and 1.0%), reported by Navarrete (1991).

Visualization of Iron Oxide Suspension Structures Under Settling

Higher magnification time-lapse videotape recordings of the settling process were conducted in order to visualize the evolution of the particle structures under gravity. The recordings of the 1.0% suspensions provided valuable information on the microstructural behavior of the suspension, showing flow of flocs, floc aggregation, and breakup during the collapse of the particle-rich layer. The high magnification experiments also indicated the presence of entrained air within freshly dispersed suspensions. The entrained air was observed as spherical bubbles ascending through the suspension, as shown in Figure 6 for a 1.0% by volume magnetic suspension. Also, this figure shows that the effect of rising bubbles is to create paths and to flocculate the suspensions as they pass; after a few minutes several paths had been created and cracks filled with oil formed in between, as shown in Figure 7.

When the bubbles reach the oil/particle interface, they break through the interface creating holes at the settling interface and dragging some flocs and oil with them, as shown in Figure 8 for a 1.0% by volume magnetic suspension.

The holes and surface structures in the oil/particle interface were observed at all concentrations and remained unchanged once formed, except for the 1.0% suspension where the collapse of the particle-rich region destroyed those structures. Top view photographs were also taken of suspensions after about 1,500 h of settling. Figures 9 present top views of the interface of 1.0% and 2.3% by volume magnetic and nonmagnetic suspensions, and Figure 10 presents a top view of a 6.0% by volume nonmagnetic suspension. The photographs show that

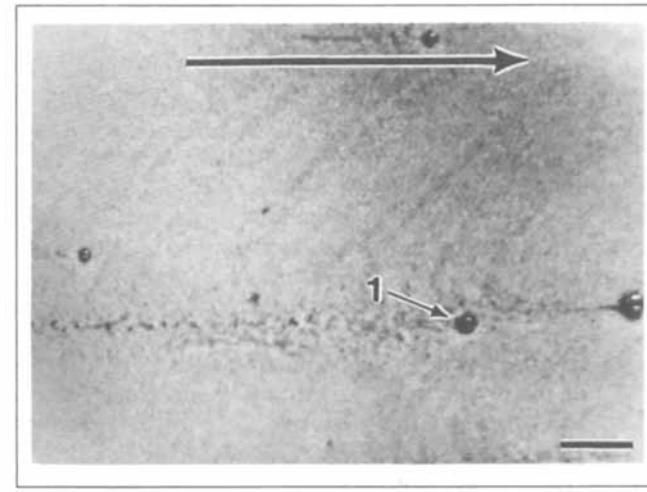

Figure 6. Air bubble ascending through a just loaded 1.0% by volume γ-Fe_2O_3 suspension (1).

Arrow indicates vertical direction. (Bar = 0.5 mm).

the holes and surface structures resemble little volcanoes, with a central hole and a surrounding mountainous region. At lower concentrations the holes become smaller and more numerous, and the surface texture of the interface between oil-rich and particle-rich regions becomes very fine and grainy between holes. Figure 11 shows a higher magnification picture of the volcano type of structures of these holes in a 3.3% by volume magnetic suspension.

The effect of air bubbles was determined by means of settling experiments with degassed suspensions. Magnetic suspensions of 1.0% and 3.3% by volume settled in a double chamber 20-mm-diameter test tube (Navarrete, 1991). A small vacuum was applied to the tube until all entrained air was removed. The void left by the departed air was filled with degassed suspension; three 3-mm-diameter nonmagnetic balls aided in dispersing the suspension. After mixing, vacuum was applied a second time to detect the presence of residual air. If no air

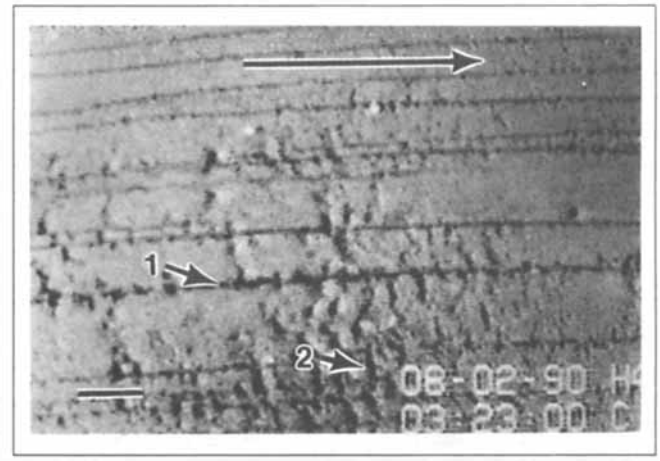

Figure 7. Paths created by ascending air bubbles (1) through a 1.0% by volume γ-Fe_2O_3 suspension before collapse at indicated time.

Horizontal cracks created between bubble paths (2). Arrow indicates vertical direction. (Bar = 0.5 mm).

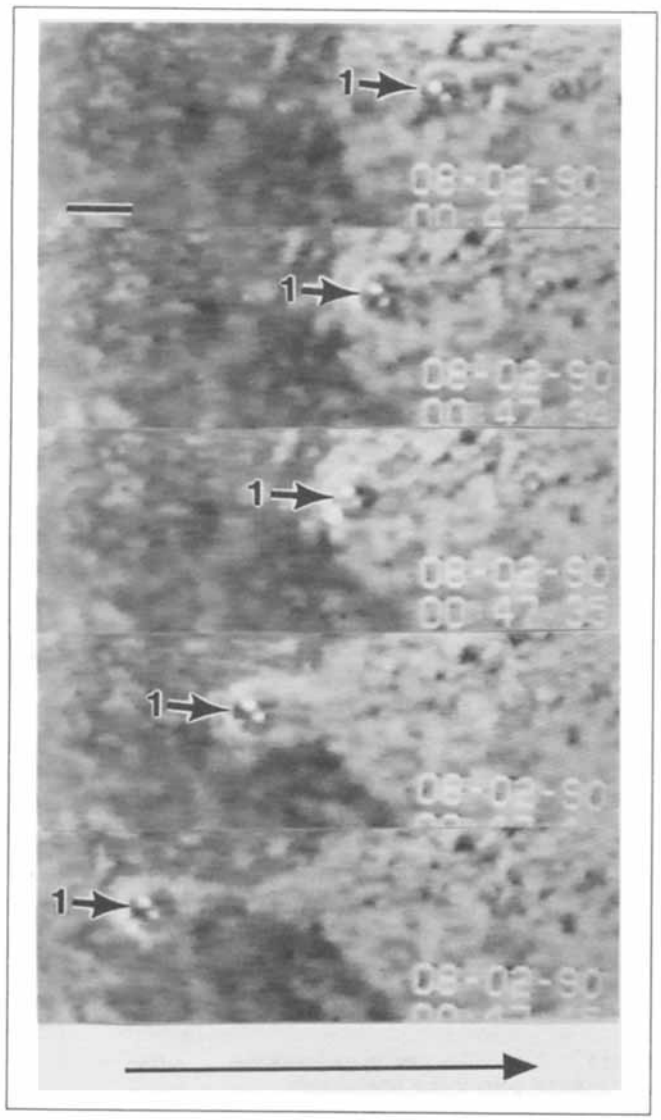

Figure 8. Sequence of a bubble (marked with 1 and arrow) breaking through the settling interface of a 1.0% by volume γ-Fe_2O_3 suspension after 47 min of settling.

(Bar = 0.3 mm).

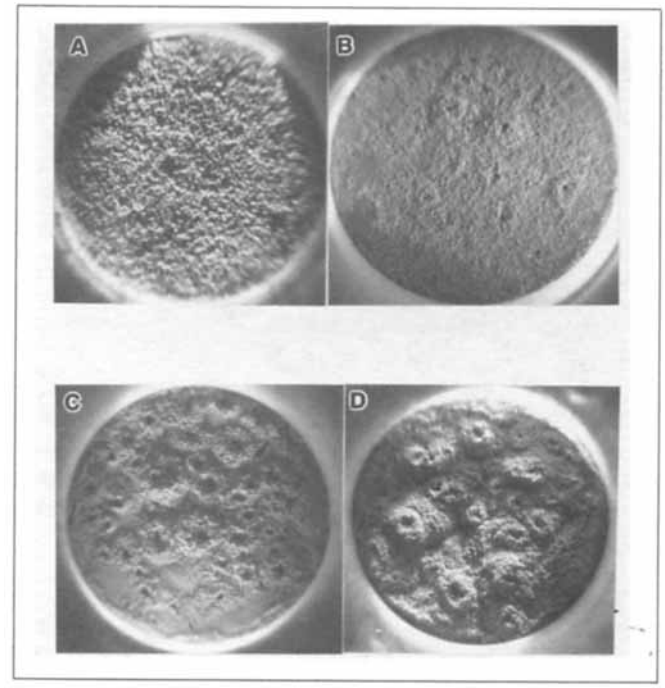

Figure 9. Top view of test tubes after about 1,500 h of settling of Fe_2O_3 suspensions (tube diameters are all 20 mm).

(A) and (C) are 1.0% and 2.3% magnetic respectively; (B) and (D) are 1.0% and 2.3% nonmagnetic respectively.

was detected, the tube was opened to atmospheric pressure and the settling process was recorded.

A comparison between the settling curves for 3.3% and 1.0% by volume magnetic suspensions that had been degassed is not shown in Figure 12. Settling was significantly retarded in the 3.3% by volume suspension and the characteristic collapse was delayed by up to 55 h for the 1.0% by the volume suspension. In this last case, the settling curves of the degassed suspensions showed significant variation among themselves, indicating that the bubbles helped regularize the collapse.

Analysis of Settling Results

Final settling properties

The compressive strain at the end of settling (that is, as time goes to infinity, extrapolated from Figure 1) is shown in Figure 13 as a function of the initial particle volume fraction ϕ_p^i of magnetic and nonmagnetic suspensions. For all ϕ_p^i's the magnetic suspensions compressed to a larger extent.

From a simple mass balance it is possible to calculate the final particle volume fraction in the particle-rich region, since the mass of particles is the same at the beginning and at the end of the settling experiment in the particle-rich region, that is,

Figure 10. Top view of a test tube after about 1,500 h of settling of a 6.0% by volume α-Fe_2O_3 suspension.

Tube diameter is 20 mm.

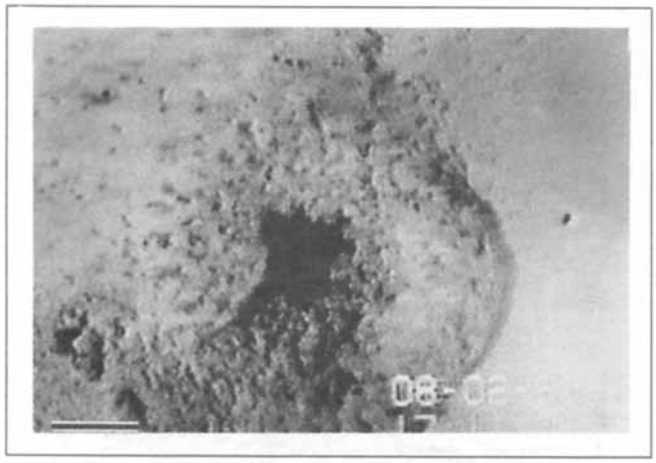

Figure 11. Close-up views of 'craters' on settling surface of a 3.3% by volume γ-Fe_2O_3 suspension after 17 h of settling.

(Bar = 2 mm).

$$V_i\Phi_p^i = V_f\Phi_p^f \tag{2}$$

where
V_i = initial particle-rich volume
V_f = final particle-rich volume
Φ_p^f = final particle volume fraction

with $V = AH$, where A = cross-sectional area of tube, and H = particle-rich settling height. Equation 2 can be written as

$$\Phi_p^f = \Phi_p^i \frac{H_o}{H_f} = \frac{\Phi_p^i}{\epsilon_c^f} \tag{3}$$

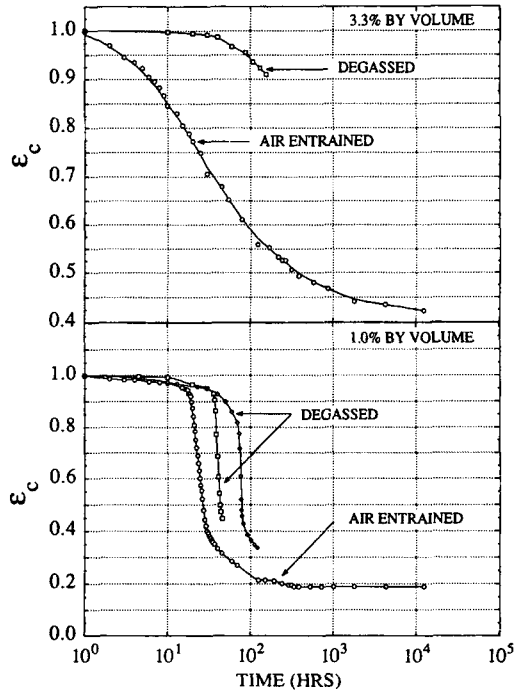

Figure 12. Comparison of settling curves of degassed and not degassed γ-Fe_2O_3 suspensions of indicated concentrations.

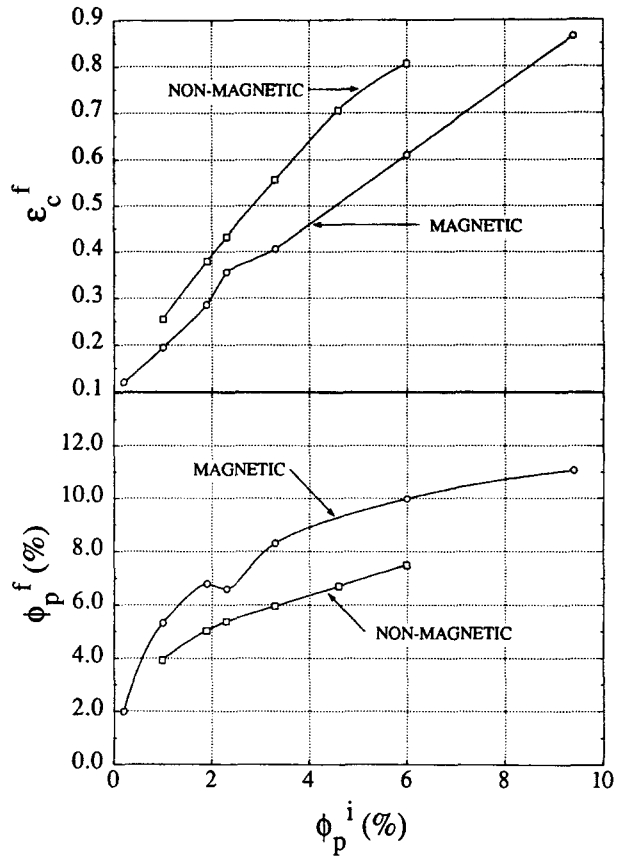

Figure 13. Comparison of final compressive strain and final particle volume fraction vs. initial particle volume fraction between magnetic and nonmagnetic iron oxide suspensions.

where
H_o = initial particle-rich phase height
H_f = final particle-rich phase height
ϵ_c^f = final compressive strain

The values of ϕ_p^f for magnetic suspensions are all larger than those of their nonmagnetic counterparts for the same particle volume fraction, shown in Figure 13.

The particle volume fraction can be expressed in terms of the floc volume fraction and the particle volume fraction per floc as

$$\Phi_p = \Phi_F\Phi_{pF} \tag{4}$$

where
Φ_F = volume fraction of flocs in suspension
Φ_{pF} = volume fraction of particles per floc,

ϕ_{pF}^f can be calculated by replacing Eq. 4 in Eq. 3 for ϕ_p^f, provided that it is assumed that in the final settled state flocs are randomly packed (ϕ_F^f = random maximum packing fraction = 64%)

$$\Phi_{pF}^f = \frac{\Phi_p^i}{0.64\epsilon_c^f} \tag{5}$$

The relative density of magnetic and nonmagnetic flocs is given by

Table 1. Particle Volume Fraction per Floc for Magnetic and Nonmagnetic Fe_2O_3 Suspensions

ϕ_p^i (%)	$(\phi_{pF}^f)_M$ (%)	$(\phi_{pF}^f)_{NM}$ (%)	$(\phi_{pF}^f)_M/(\phi_{pF}^f)_{NM}$ (%)
9.4	17.3	—	—
6.0	15.9	11.6	1.37
4.6	—	10.0	—
3.3	12.3	9.4	1.31
2.3	11.2	8.6	1.34
1.9	10.6	8.0	1.32
1.0	8.2	6.2	1.32
0.2	3.1	—	—

$$\frac{(\Phi_{pF}^f)_M}{(\Phi_{pF}^f)_{NM}} = \frac{(\epsilon_c^f)_{NM}}{(\epsilon_c^f)_M} \tag{6}$$

where the subscripts M and NM indicate magnetic and nonmagnetic respectively. The resulting final volume fraction of particles per floc and magnetic vs. nonmagnetic floc density ratios are presented in Table 1. The particle density of flocs increases with initial particle volume fraction. This shows that flocs are forced to compress—at high ϕ_p's—or interpenetrate—at low ϕ_p's—with increasing particle concentration. Also, magnetic flocs are an average of 1.32–1.37 times denser than their nonmagnetic analogs, an effect only attributable to the magnetic forces. These results are extrapolable to the initial unsettled state provided flocs do not compress or interpenetrate with each other during settling. In that case $\phi_{pF}^i = \phi_{pF}^f$, that is, the initial volume fraction of particles per floc can be made equal to the final volume fraction of particles per floc. In reality, however, some degree of interpenetration and/or compression occurs between flocs, thus $\phi_{pF}^i < \phi_{pF}^f$.

Analysis of possible mechanisms of settling of iron oxide suspensions

The following discussion focuses on the structural-level mechanisms that occur during the settling process of iron oxide suspensions documented in the previous sections.

At the initiation of settling, the suspension is homogeneous and well dispersed. The suspension begins to settle homogeneously driven by the net weight (the force of gravity minus the buoyancy force) of the particle network and opposed by the compressive strength (minimum stress above which the capacity to resist elastically compressional deformations ceases) of the particle network, the viscous drag exerted by the oil on the particles, and the shear stress arising from friction with the tube walls.

Two phenomena take place as settling proceeds:

(1) Air bubbles begin to form channels through which oil and small flocs rise. Bubbles rise all the way to the settling interface and the oil runs preferentially through these channels.

(2) Particles begin to flocculate and the space they leave free—cracks—is occupied by the rising oil, some of it diverted from the vertical channels created by the bubbles. This oil may become entrapped temporarily or indefinitely in the cracks depending on whether the particular crack becomes interconnected later on with an oil path that leads to the settling front. Some oil may also be squeezed out from the cracks in the final stages of settling during compaction.

The horizontal nature of the cracks apparently is due to the opposing effect of gravity that pulls the particles downward and the pressure of the oil in the crack that tends to keep the crack open. Cracks appear first at the top where the weight of the column of particles above them is lower. However, as particle flocculation proceeds, cracks appear at lower heights due to the increasing extent of the particle flocculation. Cracks continue to propagate downward creating interconnections between them and causing the settling velocity to increase.

During the same time, the particle concentration rises in the particle-rich region, especially in the bottom of the tube; thus the compressive strength of the particle network grows, and so do the supporting forces. Since the net weight of the particles in the particle-rich region remains about constant during settling—the rise in particle concentration is compensated by the fall of the height of the particle-rich region—the net result is that the settling rate decreases with time. This causes the S-shape of the settling curves.

The collapse of the particle-rich region observed in the low concentration suspensions (1.0% by volume magnetic and nonmagnetic suspensions and 0.2% by volume magnetic suspension), with the recirculation and backflow behavior described above, can be explained by the low compressive strength of the particle network at these concentrations, which is not sufficient to support the high particle density regions created by the flocculation and cracking process. These regions settle much faster than the rest of the particle network due to their large effective diameter and higher density, and displace lower particle density regions upward.

On the other hand, the initial settling rate of low concentration suspensions is significantly lower than that of their immediately higher concentration counterparts ($\phi_p^i = 1.9\%$, 2.3% and 3.3% magnetic, and 1.9% and 2.3% nonmagnetic). However, inspection of the settling curves of the degassed suspensions (Figure 12) indicates the initial settling rate of $\phi_p^i = 1.0\%$ is higher than $\phi_p^i = 3.3\%$. This shows that entrained gas may be the cause of the observed higher initial settling rates of suspensions with $\phi_p^i > 1.0\%$. Figure 12 also indicates that the effect of air bubbles is more important at higher concentrations than at low concentrations.

During the last part of the settling process the settling rate falls with time, flocs mainly consolidate and inter- and intrafloc oil is squeezed out through the remaining flow paths to the settling front. The larger final floc density with increasing ϕ_p^i computed from the final settled structures, Table 1, indicates that more intra-floc oil is expelled from the particle-rich region at higher concentrations as a consequence of the larger net weight of the particle network.

Summary

The visualizations of flocculated suspensions confirm to a large extent the phenomenological model proposed by Somasundaran and coworkers for slimes.

The large density difference between particles and oil in the iron oxide dispersions cause separation under gravity. Both magnetic and nonmagnetic suspensions demonstrate the following general settling trends (chronological order):

(1) Slow settling rate after loading the suspension; the duration of this slow settling period increases with increasing concentration.

(2) The settling rate increases for a period of time. The duration of this period is shorter, the lower the concentration.

(3) The settling rate slows and the system approaches a state in which no further settling under gravity occurs.

(4) The effect of air bubbles is to accelerate settling and is larger the higher the concentration of particles.

At low concentrations, the settling curves for magnetic and nonmagnetic suspensions are similar; however, the ratio of the final settled height to the total initial height is larger for nonmagnetic suspensions indicating that magnetic flocs have a higher particle floc density, about 1.3–1.4 times larger than that of their nonmagnetic analogs. This ratio is constant from 1 to 6% by volume of iron oxide.

Both magnetic and nonmagnetic suspensions form surface structures and holes in the interface between the oil-rich and particle-rich region due to the escape of entrained gas in the form of bubbles. The holes decrease in size and the surface texture becomes very fine grains (as opposed to solid-like and smooth at higher concentration) as concentration decreases.

Acknowledgment

This research was supported by the Center for Interfacial Engineering here sponsored by the National Science Foundation and industrial members.

Literature Cited

Allen, T., "Photocentrifuges," *Powder Technol.*, **50**, 193 (1987).

Allen, T., and P. H. T. Uhlherr, "Nonhomogeneous Sedimentation in Viscoelastic Fluids," *J. Rheol.*, **33**(4), 627 (1989).

Ansell, G. C., and E. Dickinson, "Brownian-Dynamics Simulation of the Formation of Colloidal Aggregate and Sediment Structure," *Faraday Discuss. Chem. Soc.*, **83**, 167 (1987).

Ayoub, A., G. E. Klinzing, and J. M. Ekmann, "Effect of Particle Size and Shape on Settling Using an Integral Approach," *Powder Technol.*, **35**, 63 (1983).

Brady, J. F., R. J. Phillips, J. C. Lester, and G. Bossis, "Dynamic Simulation of Hydrodynamically Interacting Suspensions," *J. Fluid Mech.*, **195**, 257 (1988).

Buscall, R., "The Elastic Properties of Structured Dispersions: A Simple Centrifuge Method of Examination," *Colloids Surf.*, **5**, 269 (1982).

Buscall, R., and L. White, "The Consolidation of Concentrated Suspensions," *J. Chem. Soc. Faraday Trans.*, **83**, 873 (1987).

Buscall, R., "The Sedimentation of Concentrated Colloidal Suspensions," *Colloids Surf.*, **43**, 33 (1990).

Davies, R., and B. Kaye, "Experimental Investigation into the Settling Behavior of Suspensions," *Powder Technol.*, **5**, 61 (1971).

Dickinson, E., and J. Parker, "Brownian Encounters in a Polydisperse Sedimenting System of Interacting Colloidal Particles," *J. Colloid. Interface Sci.*, **97**, 220 (1984).

Dickinson, E., "Structure of Simulated Colloidal Deposits," *Colloids and Surf.*, **39**, 143 (1989).

Gaudin, A. M., M. C. Fuerstenau, and S. R. Mitchell, "Effect of Pulp Depth and Initial Pulp Density in Batch Thickening," *Mining Eng.*, **11**, 613 (1959).

Harris, C. C., P. Somasundaran, and R. R. Jensen, "Sedimentation of Compressible Materials: Analysis of Batch Sedimentation Curve," *Powder Technol.*, **11**, 75 (1975).

Hietala, S. L., and D. M. Smith, "Porosity Effects on Particle Size Determination via Sedimentation," *Powder Technol.*, **59**, 141 (1989).

Howe, A., and M. Robins, "Determination of Gravitational Separation in Dispersions from Concentration Profiles," *Colloids and Surf.*, **43**, 83 (1990).

Huang, Y. B., and P. Somasundaran, "Discrete Modeling of Sedimentation," *Phys. Rev. A.*, **38**(12), 6373 (1988).

Koch, D., and E. Shaqfeh, "The Instability of a Dispersion of Settling Spheroids," *J. Fluid Mech.*, **209**, 521 (1989).

Michaels, A. S., and J. C. Bolger, "Settling Rates and Sediment Volumes of Flocculated Kaolin Suspensions," *I&EC Fundam.*, **1**(1), 24 (1962).

Nagaraj, D. R., L. McAllister, and P. Somasundaran, "Subsidence of Suspensions of Phosphatic Slime and Its Major Constituents," *Int. J. Mineral Processing*, **4**, 111 (1977).

Navarrete, R. C., "Rheology and Structure of Flocculated Suspensions," PhD Thesis, University of Minnesota, Minneapolis (1991).

Phillips, R. J., J. F. Brady, and G. Bossis, "Hydrodynamic Transport Properties of Hard-sphere Dispersions. II. Porous Media," *Phys. Fluids*, **31**(12), 3473 (1988).

Shih, Y. T., D. Gidaspow, and D. T. Wasan, "Hydrodynamics of Sedimentation of Multisized Particles," *Powder Technol.*, **50**, 201 (1987).

Somasundaran, P., Y. B. Huang, and C. C. Gryte, "CAT Scan Characterization of Sedimentation and Flocs," *Powder Technol.*, **53**, 73 (1987).

Somasundaran, P., E. L. Smith, Jr., and C. C. Harris, "Dewatering of Phosphate Slimes Using Coarse Additives," *Proc. 11th Int. Mineral Processes Congr.*, **49**, 1301 (1975).

Somasundaran, P., "Thickening or Dewatering of Slow-Settling Mineral Suspensions," in *Mineral Processing*, J. Laskowski, ed., 13th International Mineral Processing Congress, Warsaw, Elsevier, Amsterdam, **2**, Part A, p. 233–262 (1981).

Tiller, F. M., and Z. Khatib, "The Theory of Sediment Volumes of Compressible, Particulate Structures," *J. Colloid. Interface Sci.*, **100**(1), 55 (1984).

Utsugi, H., A. Endo, N. Suzuki, and K. Ono, "Surface-Treatment of Ceramic Powders and their Surface Properties. III. The Surface-Treatment of γ-Hematite with Alkoxysilane and their Surface Properties," *J. Japan Soc. Powder and Powder Metallurgy*, **32**, 100 (1985).

Wedlock, D. J., I. J. Fabris, and J. Grimsey, "Sedimentation in Polydisperse Particulate Suspensions," *Colloids Surf.*, **43**, 67 (1990).

Yang, M. C., L. E. Scriven, and C. W. Macosko, "Some Rheological Measurements on Magnetic Iron Oxide Suspensions in Silicone Oil," *J. Rheol.*, **30**(5), 1015 (1986).

Manuscript received July 6, 1992, and revision received Oct. 26, 1992.